Preparation of helical nanostructures using chiral cationic surfactants

Yonggang Yang, Masahiro Suzuki, Sanae Owa, Hirofusa Shirai and Kenji Hanabusa*

Received (in Cambridge, UK) 8th June 2005, Accepted 5th July 2005
First published as an Advance Article on the web 5th August 2005
DOI: 10.1039/b508106h

Left-handed helical short nanotubes and mesoporous nanofibers were prepared by sol–gel transcription using a new chiral cationic surfactant.

Recently the control of the morphologies of nanoparticles on the nano- and macro-scales has become a hot topic. The helical morphologies[1] should be the most interesting ones, because they may be used in the fields of chiral selectivity, chiral recognition, and chiral catalysis. Nanotubes have attracted many researchers, because they are superior to other nanostructures due to the fact that their borders, inner and outer surfaces could be functionalized.[2] For the preparation of silica nanotubes, the sol–gel transcription[3] method has often been selected. Different kinds of helical tubular structure have been found, *i.e.*, single-strand helical nanotubes, double helical nanotubes, helical bundles,[4] and inner-helical structure.[5] Short nanotubes may be preferred as the stationary phase in chromatography or as catalysts. Although the morphologies of nanotubes obtained by sol–gel transcription process can be monodisperse, the nanotubes are usually not uniform in size. Indeed, it is hard to control the length of the obtained nanotubes.

It was found that nanotubes could be obtained using cationic surfactants.[6] On the basis of the proposed preparation mechanism, it is hard to prepare nanotubes with helical structure or other interesting properties. Therefore, it is better to develop a new kind of compound which combines the superior properties of both surfactants and gelators, which can control both morphologies and size. Furthermore, although several papers have indicated that mesoporous silica nanofibers could be prepared using cationic surfactants,[7–11] the preparation of nanofibers with chiral pores is still a big challenge.[12–14] Here we show how to control the helical structure and helical pitch by changing solvents and the concentration of catalyst.

Compound L-**4PyCl**, which is composed of L-isoleucine, was synthesized according to Scheme 1.[15] When it was dissolved in water (10 mg L^{-1}) at room temperature, an emulsion was obtained. A polarized optical micrograph image of the emulsion suggests that vesicle-like aggregates of 2.0 μm in diameter are formed (Fig. 1a). When 0.1 mL of ethanol was dropped into this emulsion, a transparent viscous solution was obtained. The increase of viscosity indicated that the vesicle-like aggregates were changed into huge fibrous aggregates. After evaporating the mixture of water and ethanol, a three-dimensional network was observed (Fig. 1b).

Short nanotubes were synthesized according to the following procedure. The compound L-**4PyCl** (150 mg) was dissolved in 15 mL of aqueous NH_3 (1.0 wt%), and then 300 mg of tetraethoxyorthosilicate (TEOS) was dropped into the strongly stirred solution at 0 °C. After TEOS was dissolved in the solution, the mixture was kept at room temperature for one day and 80 °C for four days under static conditions. Finally, the template was removed by washing with methanol and calcination was performed at 250 °C for 2 h and 550 °C for 5 h under aerobic conditions.

Fig. 2a and 2b show both SEM and TEM images of the calcined silica nanotubes. These nanotubes were 200–300 nm in length and around 15 nm in inner diameter. Some left-handed helical nanotubes were identified from SEM image, an even 10 nm thickness of metal covered the surface for preparing the SEM specimen. The TEM image also indicated some helical character, because the inner structure of these nanotubes were not straight. It is assumed that short aggregates of compound L-**4PyCl** should act as the template. Although only the vesicle-like aggregate were

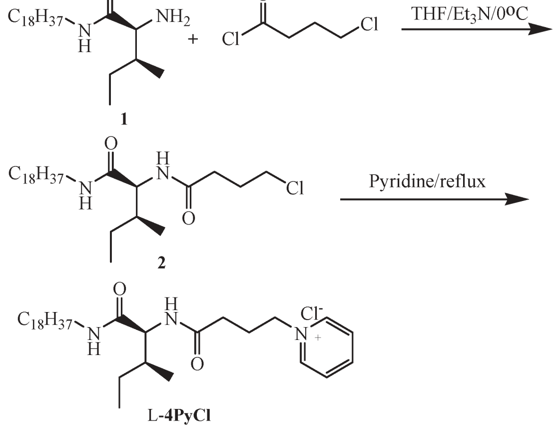

Scheme 1 Synthesis of chiral cationic surfactant L-**4PyCl**.

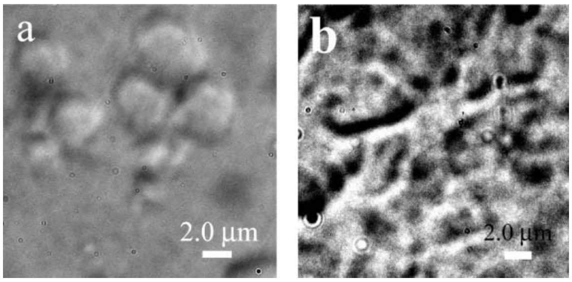

Fig. 1 (a) Polarized optical micrograph images of L-**4PyCl** aq. solution at rt (10 mg in 1 mL of H_2O); (b) Polarized optical micrograph images of dry L-**4PyCl** (prepared from the solution of L-**4PyCl** 10 mg in the mixture of 1 mL of H_2O and 0.1 mL of ethanol).

Department of Functional Polymer Science, Faculty of Textile Science and Technology, Shinshu University, Ueda, 386-8567, Japan.
E-mail: hanaken@giptc.shinshu-u.ac.jp

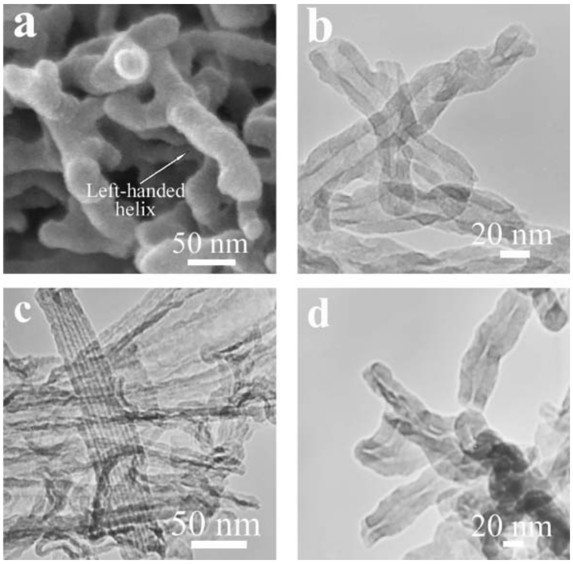

Fig. 2 (a) SEM and (b) TEM images of calcined nanotubes prepared in 1.0 wt% NH_3 aq. solution (10 mg L-**4PyCl**: 1.0 mL NH_3 aq. : 20 mg TEOS); (c) TEM image of calcined nanotubes prepared in 5.0 wt% NH_3 aq. solution (10 mg L-**4PyCl**: 1.0 mL NH_3 aq. : 20 mg TEOS); (d) TEM image of calcined nanotubes prepared in 11.3 wt% NH_3 aq. solution (10 mg L-**4PyCl**: 1.0 mL NH_3 aq.: 20 mg TEOS).

identified from polarized optical micrograph image in the aqueous solution of compound L-**4PyCl** (Fig. 1a), ethanol generated by hydrolyzing TEOS would support the formation of aggregates (Fig. 1b).

For a better understanding of this structure transcription process, we studied the effect of the catalyst concentration. Although L-**4PyCl** can dissolve in hot 2 M HCl aq. to form a transparent viscous solution, unfortunately, it precipitates out during cooling down to room temperature. Therefore, the structure transcription reaction was only carried out in base condition. When the concentration of NH_3 is 5.0 wt%, the morphologies of obtained silica became complicated. Ribbons, mesoporous fibers and inner helical nanotubes[5] were identified from both SEM and TEM image (Fig. 2c). When the concentration of NH_3 is 11.3 wt%, it is possible to observe mesoporous ribbons combined with some ultrathin inner-helical nanotubes (Fig. 2d). The nanotubes were apparently thinner than those obtained in weaker base conditions. These results indicated that uniform short helical nanotubes could be obtained only in weak base condition. With the increasing of the concentration of NH_3, mesoporous ribbons are feasible to be formed.

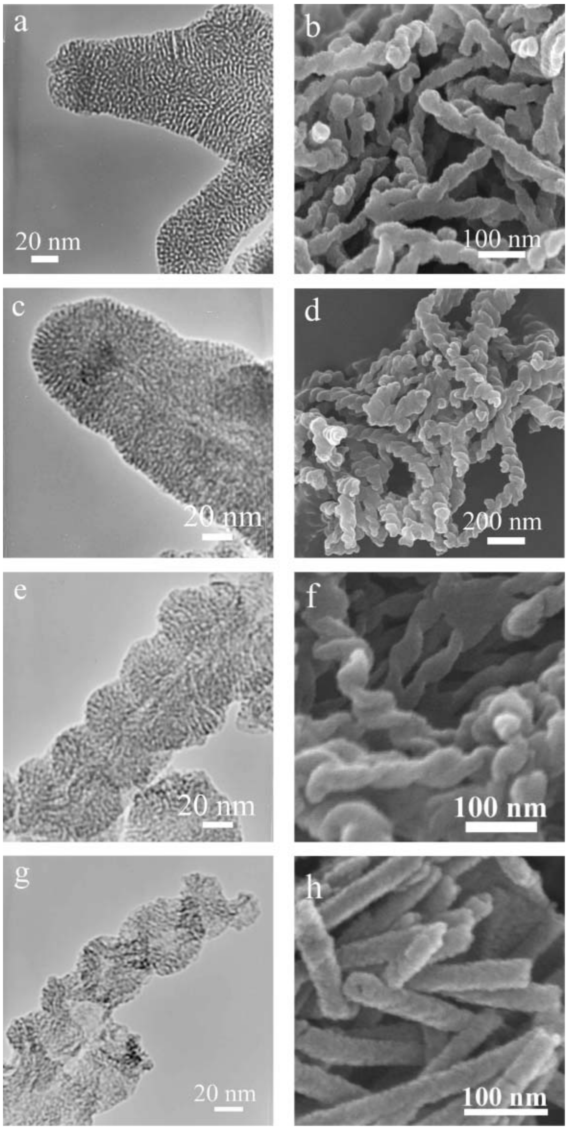

Fig. 3 (a) TEM image of calcined mesoporous silica nanofibers (preparation condition: (10 mg L-**4PyCl**: 0.9 mL 1.0 wt% NH_3 aq. : 0.1 mL ethanol : 20 mg TEOS)); (b) SEM and (c) TEM images of calcined mesoporous silica nanofibers (Preparation condition: (10 mg L-**4PyCl**: 0.6 mL 1.0 wt% NH_3 aq. : 0.4 mL ethanol : 20 mg TEOS)); (d), (f) SEM and (e), (g) TEM images of calcined mesoporous silica nanofibers (preparation condition: (10 mg L-**4PyCl**: 0.7 mL 11.3 wt% NH_3 aq. : 0.3 mL ethanol : 20 mg TEOS)). (h) SEM image of calcined mesoporous silica nanofibers (Preparation condition: (10 mg L-**4PyCl**: 0.5 mL 1.0 wt% NH_3 aq. : 0.5 mL ethanol: 20 mg TEOS)).

Since ethanol could affect the structure of the self-assemblies of L-**4PyCl**, the sol-gel transcriptions using the mixture of water and ethanol were carried out. Fig. 3 shows TEM and SEM images of calcined silica obtained at the different conditions; the concentration of NH_3 was varied from 1.0 to 11.3 wt% and the volume ratio between water and ethanol was changed from 9 : 1 to 4 : 6. When the ratio between water and ethanol was 9 : 1, the structure of the nanoparticles obtained was similar as those prepared in water from SEM images. But they are mesoporous particles which mesopores could be identified from TEM image (Fig. 3a). When the volume ratio between water and ethanol is higher than 6 : 4, uniform left-handed helical mesoporous silica nanofibers were obtained (Fig. 3b, 3d, and 3f). When the ratio between ethanol and water is 5 : 5, although the formation of ribbons were predominate (not shown here), straight nanotubes which were constructed by left-handed helical fibers were identified (Fig. 3h). The helical structure was sensitive to the concentration of NH_3, so that the helical pitch decreased with the increasing of the concentration of NH_3. Furthermore, double helical structure was feasible to be constructed in a weaker base condition (Fig. 3b and 3h), and single-strand twisted ribbons were preferentially formed in strong base condition (Fig. 3d and 3f). The mesopores could be recognized from TEM images (Fig. 3c, 3e, and 3g). The reason of the

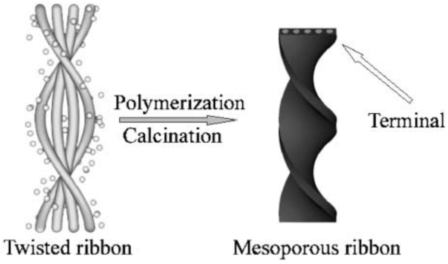

Fig. 4 The formation of left-handed mesoporous twisted ribbons.

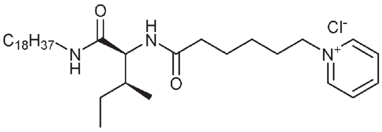

L-**6PyCl**

Fig. 5 Molecular structure of gelator L-**6PyCl**.

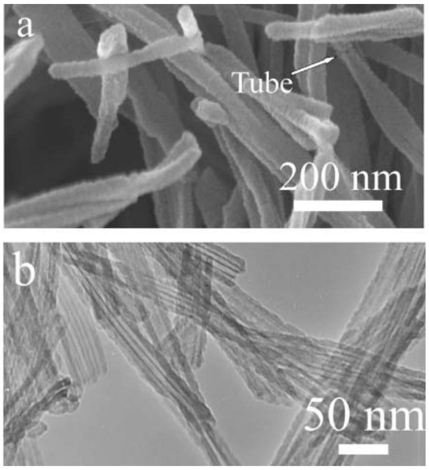

Fig. 6 (a) SEM and (b) TEM images of mesoporous twisted ribbons and tubes (Preparation condition: 10 mg L-**6PyCl**: 1.0 mL 5.0% NH_3 aq. : 20 mg TEOS).

mesopores seemed to be perpendicular to the axis of fibers is that the ribbon twisted too tightly (Fig. 3a, 3c, 3e, and 3g). The BET surface area of the silica of Fig. 3d was 729.79 $m^2 g^{-1}$ and the pore-size was around 3.8 nm. It seems that single-strand of the short fiber acted as the template (Fig. 4). The terminal image of the twisted ribbons (Fig. 3f and 3g) was also illustrated in Fig. 4.

Recently, gelators and lipids[16] have been chosen to control the morphologies of nanoparticles. To understand the difference between the gelator and the chiral cationic surfactant, gelator L-**6PyCl**, structurally related to cationic surfactant L-**4PyCl**, was selected as the structure-directing reagent (Fig. 5). The synthesis of gelator L-**6PyCl** has been published elsewhere.[15] Compound L-**6PyCl** is able to form both a hydrogel and an organogel, but not vesicle-like aggregates or viscous solution. It can gel water, cyclohexanone, THF, 1,4-dioxane, DMSO, and acetonitrile. The sol–gel transcription reaction was carried out in base. Twisted mesoporous ribbons were identified from TEM image (Fig. 6b). The tight twist resulted in tubular structure formation as shown in Fig. 6. The mesopores were running along the axes of the nanoribbons, the channels of which are 6.0 nm in inner diameter. Apparently, the silica nanofibers obtained using gelator L-**6PyCl** were longer than those obtained using surfactant L-**4PyCl**. The silica nanofibers obtained using surfactant L-**4PyCl** showed clearer helical character.

In conclusion, short left-handed helical nanotubes and left-handed helical mesoporous fibers have been synthesized by self-assembly with cationic surfactants as template. Both the helical structure and helical pitch could be modified by changing the reaction conditions.†‡

This work was supported by Grant-in-Aid for 21st Century COE Program and a grant (No. 15350132) by the Ministry of Education, Culture, Sports, Science, and Technology of Japan.

Notes and references

† SEM observations were carried out on a Hitachi S-5000 field emission scanning electron microscope (FE-SEM) at 10 kV with 10 nm metal coating. TEM observations were carried out on a JEOL JEM-2010 transmission electron microscope at 200 kV.

‡ Compound L-**4PyCl**: FT-IR (KBr): 3286 cm^{-1} (νN–H, amide A), 1635 cm^{-1} (νC=O, amide I), 1548 cm^{-1} (δN–H, amide II). ^{1}H-NMR (400 MHz, DMSO-d_6, TMS, 25 °C): $\delta = 0.71$–0.87 (m, 9H; CH_3), 1.23 (br, 32H; alkyl), 1.36–1.42 (m, 2H; $CONHCH_2CH_2$), 1.62–1.69 (m, 1H; $CH_3CH(CH_3CH_2)$), 2.13–2.18 (m, 2H; CH_2CONH), 2.22–2.26 (m, 2H; $PyCH_2CH_2$), 2.91–3.14 (m, 2H; $CONHCH_2$), 4.08 (t, J = 8.6 Hz, 1H; NHC*H*CO), 4.57–4.61 (m, 2H; CH_2Py), 7.97 (d, J = 8.8 Hz, 1H; CON*H*CH), 8.01 (t, J = 5.6 Hz, 1H; $CCNHCH_2$), 8.16 (t, J = 7.6 Hz, 2H; 3-Py*H*), 8.61 (t, J = 7.6 Hz,1H; 4-Py*H*), 9.10 (d, J = 5.6 Hz, 2H; 2-Py*H*). elemental analysis: $C_{33}H_{60}ClN_3O_2$ (M_w; 566.30), calcd (%): C, 69.99; H, 10.68; N, 7.42. found: C, 70.23; H, 11.00; N, 7.41.

1 T. E. Gier, X. Bu, P. Feng and G. D. Stucky, *Nature*, 1998, **395**, 154.
2 G. R. Patzke, F. Krumeich, R. Nesper and G. A. Stucky, *Angew. Chem. Int. Ed.*, 2002, **41**, 2446.
3 Y. Ono, K. Nakashima, M. Sano, Y. Kanekiyo, K. Inoue, J. Hojo and S. Shinkai, *Chem. Commun.*, 1998, 1477.
4 J. H. Jung, Y. Ono, K. Hanabusa and S. Shinkai, *J. Am. Chem. Soc.*, 2000, **122**, 5008; J. H. Jung, Y. Ono and S. Shinkai, *Chem. Eur. J.*, 2000, **6**, 4552; A. M. Seddon, H. M. Patel, S. L. Burkett and S. Mann, *Angew. Chem. Int. Ed.*, 2002, **41**, 2988; S. Kobayashi, N. Hamasaki, M. Suzuki, M. Kimura, H. Shirai and Kenji Hanabusa, *J. Am. Chem. Soc.*, 2002, **124**, 6550; K. Sugiyasu, S. Tamaru, M. Takeuchi, D. Berthier, I. Huc, R. Oda and S. Shinkai, *Chem. Commun.*, 2002, 1212; J. H. Jung, K. Yoshida and T. Shimizu, *Langmuir*, 2002, **18**, 8724.
5 J. H. Jung, S. Shinkai and T. Shimizu, *Chem. Mater.*, 2003, **15**, 2141.
6 M. Harada and M. Adachi, *Adv. Mater.*, 2000, **12**, 839.
7 N. Yang, N. Coombs and G. A. Ozin, *Nature*, 1997, **386**, 692; S. Mann and G. A. Ozin, *Nature*, 1996, **382**, 313.
8 H. P. Lin and C. Y. Mou, *Science*, 1996, **273**, 765; H. P. Lin, S. B. Liu, C. Y. Mou and C. Y. Tang, *Chem. Commun.*, 1999, 583.
9 S. Schacht, Q. Huo, I. G. Voigt-Martin, G. D. Stucky and F. Schüth, *Science*, 1996, **273**, 768; F. Kleitz, F. Marlow, G. D. Stucky and F. Schüth, *Chem. Mater.*, 2001, **13**, 3587; Q. Huo, D. Zhao, J. Feng, K. Weston, S. K. Buratto and G. D. Stucky, *Adv. Mater.*, 1997, **9**, 974.
10 P. J. Bruinsma, A. Y. Kim, J. Liu and J. S. Baskaran, *Chem. Mater.*, 1997, **9**, 2507.
11 F. Marlow, B. Spliethoff, B. Tesche and D. Zhao, *Adv. Mater.*, 2000, **12**, 961.
12 W. J. Kim and S. M. Yang, *Adv. Mater.*, 2001, **13**, 1191.
13 S. Che, Z. Liu, T. Ohsuna, K. Sakamoto, O. Terasaki and T. Tatsumi, *Nature*, 2004, **429**, 281.
14 Y. Yang, M. Suzuki, A. Kurose, H. Shirai and Kenji Hanabusa, *Chem. Commun.*, 2005, 2032.
15 M. Suzuki, S. Owa, M. Kimura, A. Kurose, H. Shirai and K. Hanabusa, *Tetrahedron Lett.*, 2005, **46**, 303.
16 A. M. Seddon, H. M. Patel, S. L. Burkett and S. Mann, *Angew. Chem. Int. Ed.*, 2002, **41**, 2988.